EV20/Omomyc: A novel dual MYC/HER3 targeting immunoconjugate

Sandra Bibbò [a,b,1,2], Emily Capone [a,b,2], Giulio Lovato [a,b], Sara Ponziani [c],
Alessia Lamolinara [b,c,d], Manuela Iezzi [b,d], Rossano Lattanzio [a,b], Katia Mazzocco [e],
Martina Morini [e], Francesco Giansanti [c], Vincenzo De Laurenzi [a,b], Jonathan Whitfield [h],
Stefano Iacobelli [f], Rodolfo Ippoliti [c,*****], Marie-Eve Beaulieu [g,****], Laura Soucek [g,h,i,j,***],
Arturo Sala [k,**], Gianluca Sala [a,b,*]

[a] Department of Innovative Technologies in Medicine & Dentistry, University "G. D'Annunzio" of Chieti-Pescara, Chieti, Italy
[b] Center for Advanced Studies and Technology (CAST), University "G. D'Annunzio" of Chieti-Pescara, Chieti, Italy
[c] Department of Life, Health and Environmental Sciences, University of L'Aquila, Coppito, Italy
[d] Department of Neurosciences, Imaging and Clinical Sciences, University "G. D'Annunzio" of Chieti-Pescara, Chieti, Italy
[e] Laboratory of Experimental Therap ies in Oncology, IRCCS Istituto Giannina Gaslini
[f] MediaPharma s.r.l., Via Colonnetta 50/A, Chieti, Italy
[g] Peptomyc S.L., Barcelona 08035, Spain
[h] Vall d'Hebron Institute of Oncology (VHIO), Barcelona 08035, Spain
[i] Department of Biochemistry and Molecular Biology, Universitat Autònoma de Barcelona, Bellaterra 08193, Spain
[j] Institució Catalana de Recerca i Estudis Avançats (ICREA), Barcelona, Spain
[k] Centre for Inflammation Research and Translational Medicine (CIRTM); College, of Health, Medicine and Life Sciences, Brunel University London, Uxbridge UB8 3PH,
United Kingdom,

ARTICLE INFO

ABSTRACT

MYC is one of the most important therapeutic targets in human cancer. Many attempts have been made to develop small molecules that could be used to curb its activity in patients, but most failed to identify a suitable direct inhibitor. After years of preclinical characterization, a tissue-penetrating peptide MYC inhibitor, called Omomyc, has been recently successfully used in a Phase I dose escalation study in late-stage, all-comers solid tumour patients. The study showed drug safety and positive signs of clinical activity, prompting the beginning of a new Phase Ib combination study currently ongoing in metastatic pancreatic adenocarcinoma patients.

In this manuscript, we have explored the possibility to improve Omomyc targeting to specific cancer subtypes by linking it to a therapeutic antibody. The new immunoconjugate, called EV20/Omomyc, was developed by linking a humanised anti-HER3 antibody, named EV20, to Omomyc using a bifunctional linker. EV20/Omomyc shows antigen-dependent penetrating activity and therapeutic efficacy in a metastatic model of neuroblastoma. This study suggests that directing Omomyc into specific cell types using antibodies recognising tumour antigens could improve its therapeutic activity in specific indications, like in the paediatric setting.

* Correspondence to: Gianluca Sala, Laboratory of Clinical Biochemistry and Molecular Biology, Center for Advanced Studies and Technology (CAST), Department of Innovative Technologies in Medicine & Dentistry, "G. d'Annunzio" University of Chieti-Pescara, Via L. Polacchi 11-66110, Chieti, Italy.
** Correspondence to: Arturo Sala, Centre for Inflammation Research and Translational Medicine (CIRTM), College, of Health, Medicine and Life Sciences, Brunel University London, Uxbridge UB8 3PH, United Kingdom.
*** Correspondence to: Laura Soucek, Peptomyc S.L., Barcelona 08035, Spain; Vall d'Hebron Institute of Oncology (VHIO), Barcelona 08035, Spain; Institució Catalana de Recerca i Estudis Avançats (ICREA), Barcelona, Spain. Department of Biochemistry and Molecular Biology, Universitat Autònoma de Barcelona, Bellaterra, Spain.
**** Corresponding author.
***** Corresponding author.
E-mail addresses: Rodolfo.ippoliti@univaq.it (R. Ippoliti), mbeaulieu@peptomyc.com (M.-E. Beaulieu), lsoucek@vhio.net (L. Soucek), arturo.sala@brunel.ac.uk (A. Sala), g.sala@unich.it (G. Sala).
[1] Current address for S. Bibbò: Department of Medicine and Aging Sciences, University "G. D'Annunzio" of Chieti-Pescara, Chieti, Italy.
[2] These authors contributed equally.

1. Introduction

The MYC family of transcription factors is composed of 3 members: MYC, MYCN and L-MYC. They form an essential signalling hub in most human malignancies: about 70% of all cancers display excessive MYC function as a consequence of genetic, metabolic or transcriptional deregulation in transformed cells [1]. This leads to the robust dependency of a variety of human malignancies on MYC signalling, which has been documented in both solid and haematologic cancers [2]. MYC exerts its transforming function by regulating gene expression. Evidence suggests that increased expression of MYC family members can activate specific target genes required for transformation but can also induce generalised transcriptional amplification by a phenomenon called enhancer invasion [3]. In each case, MYC activity is dependent on the interaction with a MYC-like protein called MAX. Only the MYC-MAX heterodimer can bind to DNA, promoting transcriptional activation. A mini-protein therapeutic, called Omomyc, was developed to target MYC. Omomyc is a 91-aminoacid protein derived from the MYC basic Helix-Loop-Helix leucine zipper (bHLHZ) domain that acts as a dominant negative molecule, inhibiting MYC/MYCN/L-MYC association with MAX, with positive therapeutic effects in cancer models [4]. It has been shown that systemic transgenic expression or intravenous injection of recombinant Omomyc in mice can impair the growth of different types of tumours, with only marginal effects on normal tissue homeostasis [4–6]. The same excellent safety has been recently confirmed in humans in a Phase I clinical trial (https: //clinicaltrials.gov/ct2/show/NCT04808362). A notable feature of Omomyc is its cell penetrating ability [5]. However, while its preclinical biodistribution following intravenous (i.v.) administration supported its use for the majority of solid tumours, the drug's distribution into harder-to-reach tissues (eg. brain or nerves) has not been studied yet and could limit its clinical application. To overcome these potential issues, we have explored the idea of using Omomyc as a payload of a new immunoconjugate, taking advantage of an internalising therapeutic antibody against HER3 developed by Mediapharma. This naked antibody is endowed with a moderate anticancer activity related to its ability to suppress HER3 signalling [7–12]. The antibody was later improved by linking different antineoplastic agents, generating ADCs with potent anticancer activity in a variety of HER3+ cancers, including melanoma and breast tumours [13–17]. EV20 was therefore prioritised for conjugation experiments with Omomyc.

In previous studies, it was reported that expression of HER receptor family members may represent a novel prognostic factor for paediatric cancer outcome [18,19], and in immunohistochemical analysis screenings we found that 20% of human neuroblastomas express HER3 (Natali, Iacobelli and Sala, unpublished data). Furthermore, EGFR family members, including HER3, have been shown to be expressed and involved in the proliferation of neuroblastomas [20]. Neuroblastomas, as well as other paediatric malignancies of the nervous system, are still very difficult to treat. Molecular therapies, some of which are in Phase I/II clinical trials, are based on the development of drugs targeting overexpressed or mutated signalling molecules important for neuroblastoma cell proliferation, survival or DNA repair. The ALK kinase, which is mutated or activated in about 10% of neuroblastomas, has been used as a target with different generations of ALK inhibitors with some success [21]. However, in a recent clinical trial with the third generation ALK inhibitor Lornatinib, there were fewer responses in younger patients harbouring MYCN amplified tumours, suggesting that anti-MYC strategies should be included for a better outcome of biomarker-directed precision therapies [22]. Indeed, neuroblastoma is one of the cancer types most addicted to MYC or MYCN expression [23]. MYCN is amplified in more than half of high-risk neuroblastomas, where it drives a gene expression program required for the proliferation, metabolic activity and survival of tumour cells [24]. Given the importance of targeting MYC in high-risk neuroblastoma, we elected to use this system for a proof of principle validation study of EV20/Omomyc.

2. Results

2.1. Assessment of the anticancer activity of free Omomyc against neuroblastoma cells

It has been reported that the anti-MYC mini-protein Omomyc inhibits proliferation of a wide range of cell lines expressing different levels of MYC or MYCN [4]. To confirm the anticancer activity of Omomyc in neuroblastoma cells, we quantified the anti-proliferative effect of free Omomyc in MYCN amplified (Kelly, IMR32) or non MYCN amplified (SKNAS) neuroblastoma cell lines, using 72 h as endpoint and a concentration of the peptide of 20 μM. Cells were cultured in the presence or absence of the peptide, after which cell proliferation was quantified by MTT assay. While at longer time points (i.e. two weeks) all cell lines are sensitive to MYC inhibition by Omomyc (data not shown), this short time point identifies differences in sensitivity between the MYCN amplified cancer cell lines and those with lower levels of MYC/MYCN expression. Only the IMR32 and Kelly cell lines were significantly inhibited by Omomyc, whereas the SKNAS cell line was unperturbed (Fig. 1A, left panel). Notably, sensitivity to Omomyc correlated with the expression of MYCN, but not with that of its partner protein MAX (Fig. 1A, right panel).

2.2. Expression of HER3 in human neuroblastomas tissues and generation of a neuroblastoma cell line overexpressing HER3 on the cell surface

To confirm HER3 expression in human neuroblastomas, we analysed a panel of 50 primary tumours from the Gaslini hospital by immunohistochemistry. Positivity to the HER3 antibody was cytoplasmic and detected in 48% of the samples (example staining shown in Fig. 1B), with percentages of positive tumour cells ranging from 3 to 100% (mean 60% ± 6.8). In order to evaluate the relationship between HER3 expression levels in neuroblastomas and patients' clinicopathological features, we utilized a semi-quantitative scoring system for HER3 immunohistochemical staining, based on the method reported by Izycka-Swieszewska et al. [25] HER3 levels in tumour cells were categorized as "Negative" ($n = 25$), "Low-expression" ($n = 13$), or "High-expression" ($n = 12$) and then further divided into either "Negative/Low" ($n = 38$) or "High" ($n = 12$) HER3-expressing tumours for statistical analysis. At the chi-square test, we found no significant association between HER3 expression levels and patients' clinicopathological characteristics (Table 1).

Next, we inspected a panel of patient derived and previously established neuroblastoma cell lines by western blotting with an HER3 antibody. Surprisingly, none of the cell lines showed positivity for HER3 expression (Fig. 1C). This could be a consequence of the lower expression of HER3 in neuroblastoma stages 3–4, from which neuroblastoma cell lines have been isolated, than stages 1–2 (Supplementary Fig. 1). We also noted that drug resistance caused reactivation of HER3 expression in a neuroblastoma cell line, suggesting that positive HER3 immunostaining in primary neuroblastoma samples could reflect treatments (Supplementary Fig. 2). We therefore decided to select the MYCN amplified Kelly cell line, which easily forms subcutaneous or metastatic tumours in immunodeficient mice, for genetic manipulation. Kelly cells were infected with a lentivirus containing the HER3 cDNA. After selection, the infected cell line showed strong HER3 protein expression detected by western blot analysis; expression on the cell surface was confirmed by flow cytometry (Fig. 1D).

To assess whether the EV20 antibody could engage the overexpressed HER3 molecule on neuroblastoma cells, we cultured Kelly-HER3 cells in the presence of increasing concentrations of EV20/MMAF ADC (DAR between 4 and 5), previously shown to specifically act against HER3 positive cells [16]. Low nanomolar concentrations of the ADC killed Kelly-HER3 cells with high efficiency, whereas Kelly-Mock cells were not affected (Fig. 1E), confirming that the anticancer activity of the antibody depends on HER3 expression.

2.3. Generation of an EV20/Omomyc targeting HER3

We conjugated the Omomyc molecule to EV20 and named it EV20/Omomyc. It consists of 3 domains: a) Omomyc, b) a bifunctional linker, and c) the EV20 anti-HER3 antibody (Fig. 2 A). In a nutshell, the bifunctional linker small molecule attached to the mAb enables disulfide-mediated conjugation to a C-terminal cysteine residue on the Omomyc moiety. This disulfide link gets spontaneously reduced in the cytoplasm of cells, freeing both molecular moieties.

EV20 is an antibody that is internalized very efficiently by HER-3 positive cells following the endosomal–lysosomal degradation pathway. Using different payloads and conjugation/linker chemistry we have demonstrated that EV20 is an excellent moiety for drug delivery into cancer cells [13–16,26]. The detailed procedures are described in the methods section.

Successful conjugation of the peptides was confirmed through mass spectrometry (Fig. 2B), SDS-PAGE analysis in reducing and non-reducing conditions (Fig. 2C) and anti-Omomyc or anti-human Western Blot analysis (Fig. 2D). EV20/Omomyc resulted to be conjugated with a drug-to-antibody ratio (DAR) of 1 and a percentage of residual unconjugated antibody estimated as around 50%. We then assessed if the immunoconjugate bound to HER3 with an affinity similar to the parental EV20 antibody. Both the ELISA binding assay (Fig. 2E) and flow cytometry carried out with A375m melanoma cells, expressing high levels of endogenous HER3 (Fig. 3A), confirmed that EV20/Omomyc binds HER3 antigen with an affinity comparable to the naked antibody. In order to assess EV20/Omomyc stability, we developed a sandwich anti-Omomyc ELISA using a murine anti-Omomyc as bait antibody and HRP-labelled goat anti-human IgG for the detection. The assays efficiently discriminated the EV20/Omomyc immunoconjugate from the naked EV20 antibody (Fig. 2F). Subsequently, stability of the immunoconjugate was evaluated incubating EV20/Omomyc at 37 °C in human serum for different time intervals, up to 72 h. Around 50% of the immunoconjugate was detected after 24 h of incubation (Fig. 2G).

Since Omomyc was shown to internalize into several cell types [4,5], we assessed if the EV20/Omomyc conjugate retained the same internalization capacity and could allow efficient delivery and release of the Omomyc moiety to the nuclei, where MYC exerts its functions.

Confocal microscopy confirmed that EV20/Omomyc was detected inside HER3+ A375 melanoma cells, confirming the ability of the immunoconjugate to penetrate cells (Fig. 3B). Interestingly, after EV20/Omomyc was internalized, the EV20 antibody was detected in the perinuclear/Golgi area of the cell, whereas Omomyc was localized in the nuclear compartment (Fig. 3C), suggesting their separation after penetration.

Notably, while the amount of internalized EV20/Omomyc was significantly different between Mock and HER3 transduced Kelly cells, no difference was observed in cells incubated with free Omomyc, indicating that EV20/Omomyc preferential penetration into HER3 positive cells is driven by HER3 (Fig. 4A). However, the residual amount of EV20/Omomyc observed in HER3 negative cells (Fig. 4A) probably reflects the intrinsic cell penetrating properties of Omomyc [5]. However, binding of the immunoconjugate on HER-3 negative cells is detected only at high concentration (>10 μg/ml) as also observed by flow cytometry (Fig. 4B). Indeed, to assess whether target specificity could be increased by lowering the concentration of EV20/Omomyc, a titration experiment was implemented using mock infected and HER3 expressing Kelly cells. We observed that lowering the concentration of EV20/Omomyc to 0.2 μg/ml highlighted the specificity of the immunoconjugate for HER3 positive NB cells (Fig. 4C).

2.4. Anticancer activity of EV20/Omomyc

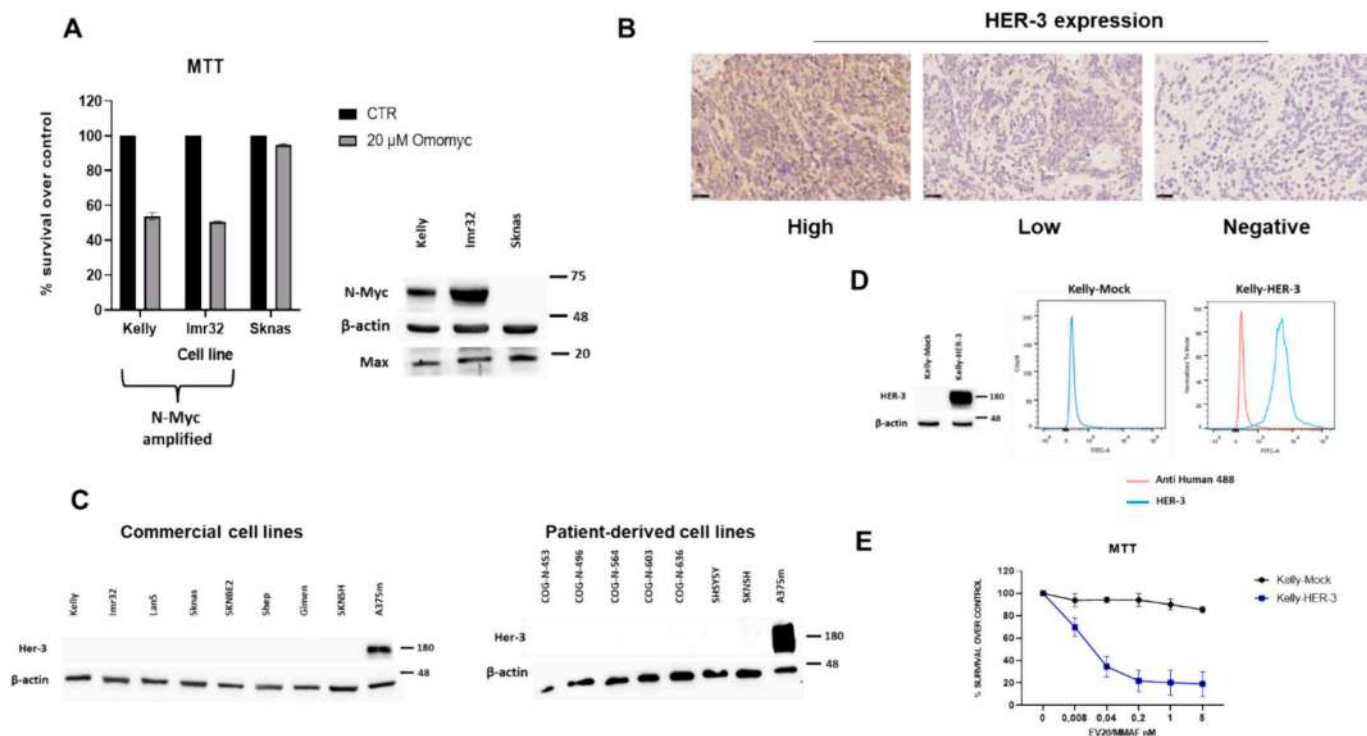We recently established a pseudo-metastatic neuroblastoma model

Fig. 1. Generation of HER3 overexpressing neuroblastoma cells.
(A) A panel of neuroblastoma cell lines were treated for 72 h with 20 μM of Omomyc and cell viability measured by MTT staining (left panel). Expression of MYCN/MAX was assessed by western blotting; a beta actin antibody was used to verify equal protein loading (right panel); (B) Examples of high, low, and negative HER3 IHC expression levels in human neuroblastoma tissues; (C) Commercially available and patient-derived cell lines were analysed for HER3 expression by western blotting. Melanoma A375m cells were used as a positive control; (D) Flow cytometry analysis and western blotting showing HER3 overexpression in Kelly-HER3 cells. (E) Cell proliferation assay showing Kelly-HER3 sensitivity to EV20/MMAF ADC. Error bars indicate standard deviations.

Table 1
HER3 status according to clinicopathological features of NB patients.

Variable	HER3		P*
	Negative/Low: n (%)	High: n (%)	
Age			
≤ 18 months	13 (72.2)	5 (27.8)	
> 18 months	25 (78.1)	7 (21.9)	0.735
Gender			
Male	15 (71.4)	6 (28.6)	
Female	23 (79.3)	6 (20.7)	0.738
Tumour location			
Adrenal	23 (82.1)	5 (17.9)	
Extra-adrenal	15 (68.2)	7 (31.8)	0.324
Tumour stage			
Localized	17 (70.8)	7 (29.2)	
Metastatic	21 (80.8)	5 (19.2)	0.514
Tumour differentiation			
Undifferentiated	2 (66.7)	1 (33.3)	
Poorly differentiated	31 (75.6)	10 (24.4)	
Differentiating	3 (100)	0 (0.0)	0.576
MYCN			
Nonamplified	16 (69.6)	7 (30.4)	
Amplified/Gain	19 (79.2)	5 (20.8)	0.517
Tumour relapse			
No	27 (75.0)	9 (25.0)	
Yes	11 (78.6)	3 (21.4)	1.000
Prognostic Group			
Very low	7 (53.8)	6 (46.2)	
Low	5 (100)	0 (0.0)	
Intermediate	3 (75.0)	1 (25.0)	
High	23 (82.1)	5 (17.9)	0.129
Patient Survival			
Alive	25 (75.8)	8 (24.2)	
Dead	10 (90.9)	1 (9.1)	0.411

*Pearson's χ^2 test.

based on intravenous injections of Kelly cells [27,28]. Firstly, we used this model to confirm that HER3 modified Kelly cells were sensitive to EV20/MMAF ADC [16], previously shown to inhibit HER3 positive cancers. As expected, the EV20/MMAF ADC showed a strong anti-metastatic activity against Kelly-HER3 cells, but it was unable to antagonise the growth of control vector-infected Kelly cells in vivo (Fig. 5A). Next, we assessed the metastatic growth of Kelly-HER3 cells in mice injected intravenously with Omomyc (0.6 mg/Kg), EV20 (5 mg/Kg), or EV20/Omomyc (5 mg/Kg) compared to sham injected, control mice. It should be noted that the free Omomyc concentration used in these experiments (0.6 mg/Kg) is approximately 50 times less than that previously used in preclinical in vivo experiments with the naked Omomyc [5] and it is about 4 times higher than the amount of Omomyc loaded in the immunoconjugate (EV20/Omomyc). Strikingly, there was a significant reduction of Kelly-HER3 metastases in the livers of mice treated with EV20/Omomyc, but not in mice treated with naked Omomyc or the anti-HER3 antibody (Fig. 5B). No reduction of liver metastases was observed in mice injected with control vector-infected Kelly cells and treated with EV20/Omomyc, naked Omomyc or EV20. In agreement with these observations, there was a target-dependent accumulation of EV20 only in Kelly-HER3 tumour tissues, demonstrating selective accumulation of EV20/Omomyc in HER3 positive cells in vivo (Fig. 5C,D).

Experimental metastasis assays performed with Kelly-Mock and Kelly-HER3 neuroblastoma cell model. (A) PBS and EV20/MMAF (10 mg/kg) intravenous injections were administered weekly for a total of 2 doses. Metastatic lesions in liver were analysed and plotted on graphs as mean number of lesions +/− SD. **$p < 0,01$ determined by Student t-test. (B) PBS, EV20 (5 mg/kg), EV20/Omomyc (5 mg/kg) and free Omomyc (0.6 mg/kg) intravenous injections were administered weekly for a total of 4 doses. Metastatic lesions in liver were analysed and plotted on graphs as mean number of lesions +/-SD. *$p = 0,03$ determined by one-way ANOVA; (C) Representative immunofluorescence images showing EV20 accumulation in tumour tissues derived by subcutaneous injection of Mock or HER3 transduced Kelly cells. After EV20/Omomyc circulated for 24 h, tumour tissues were excised and subjected to immunofluorescence staining with anti-human IgG (green); blood vessels were stained using anti CD31/CD105 antibodies (red); cell nuclei were stained by DAPI (blue); (D) Quantification of mean fluorescence intensity (MFI) of anti-human IgG performed on digital images of 3 tumours per group (5 × 400 microscopic field per sample).

3. Discussion

The Omomyc-derived therapeutic (OMO-103) is the first anti-MYC mini-protein tested in the clinic. OMO-103 recently showed safety and positive signs of drug activity in a dose-escalation study in all-comers solid tumour patients [29]. OMO-103 is now being tested in a Phase Ib study in first line metastatic pancreatic ductal adenocarcinoma patients in combination with standard of care chemotherapy (NCT06059001).

An interesting feature of Omomyc is that it possesses tissue penetrating characteristics, therefore it can enter cells and exert anticancer activity without other aids [4,5]. It has been shown in animal models that Omomyc's effects on normal tissues are only slightly antiproliferative and reversible, whereas it causes growth arrest and death in cancer tissues [6]. These preclinical results have been validated in the clinical trial, in which no severe toxicity of OMO-103 was detected in patients (manuscript under revision).

Despite the great promise of Omomyc for adult types of human cancers, the use of the drug in the paediatric setting has not been explored. In this context, improving the specific tumour tissue delivery could potentially allow for improved therapeutic index and reduce the dose required to treat a paediatric patient population. To explore this avenue, we sought to combine the anticancer activity of the Omomyc mini-protein with antibody-mediated precision targeting to generate a new, non-toxic and potentially more effective drug against hard-to-reach MYC-dependent cancers. Paediatric solid tumours are particularly susceptible to MYC inhibition, given the complete dependence of some cancer subtypes on MYC/MYCN expression, including for example medulloblastoma and neuroblastoma. In neuroblastoma, expression of HER3 was detected in 20–50% of cases in independent patient cohorts and HER3 is highly expressed in many human solid tumours, especially in the context of drug resistance [30,31]. In this study, we have taken advantage of a preclinical anti-HER3 monoclonal antibody developed in our laboratory and conjugated it to Omomyc using a bifunctional linker. However, when we looked for suitable cancer cell targets to test this therapeutic, we could not detect HER3 in commonly used neuroblastoma cell lines, nor in PDX-derived tumour cells (Fig. 1C).

To overcome this difficulty, we have transduced a classic MYCN-amplified neuroblastoma cell line (Kelly) with a lentiviral vector encoding HER3. Surface expression of HER3 made these neuroblastoma cells susceptible to killing by a previously characterised HER3 ADC, EV20/MMAF, whereas control cells were unaffected. We then used this cell model system to assess whether a HER3 antibody conjugated to Omomyc could be used to increase uptake of the drug into neuroblastoma cells expressing the receptor. Indeed, conjugation of Omomyc to the HER3 antibody dramatically increased its uptake at lower doses, reflected by its more effective anticancer activity, compared to the free
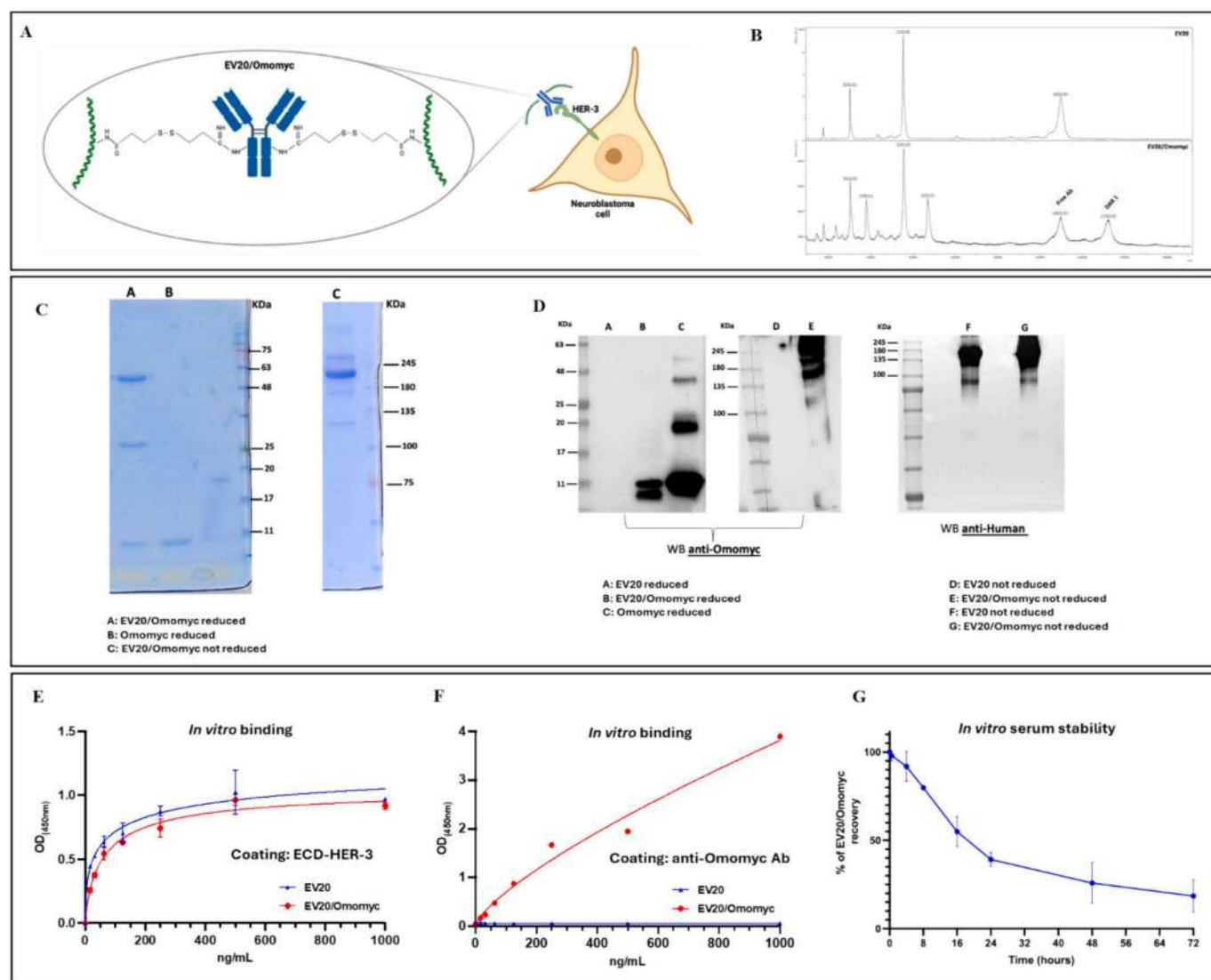
Fig. 2. Schematic structure and characterization of the EV20/Omomyc fusion protein.
Schematic structure of EV20/Omomyc; (B) Mass spectrometry analysis of naked and Omomyc-conjugated EV20; (C) Coomassie blue staining showing EV20/Omomyc in reduced and non-reduced conditions; (D) 5 μg of purified EV20/Omomyc immunoconjugate was analysed by western blotting in non-reducing (right and middle panel) and reducing conditions (left panel). Anti-Omomyc and anti-human antibodies were used as indicated; (E) in vitro binding of naked and Omomyc-conjugated EV20 antibodies. ELISA was performed using as capture antigen the HER-3 extra cellular domain (ECD) and bound EV20 or EV20/Omomyc were detected by HRP-labelled goat anti-human IgG; (F) Sandwich ELISA was performed using the murine anti-Omomyc antibody as coating and HRP-labelled goat anti-human IgG for detection; (G) in vitro stability assay performed using anti-Omomyc ELISA on human serum samples containing EV20/Omomyc incubated at 37 °C for the indicated times. Error bars indicate standard deviations.

mini-protein, in a pseudo-metastatic model of neuroblastoma. In principle, this strategy could be adapted to other paediatric cancers driven by MYC for which antibodies targeting surface antigens have been developed. In fact, MYC expression is elevated in the high risk group 3 medulloblastoma and its ectopic expression can induce aggressive growth and promote metastasis in low risk groups [32]. In rhabdomyosarcoma, MYCN is a downstream effector of the oncogenic PAX3-FOXO1 fusion protein and its destabilisation by an Aurora A kinase inhibitor has therapeutic effects in PDX models of the disease [33]. Interestingly, using publicly available databases, we found a significant correlation between expression of MYC/MYCN and HER3 in rhabdomyosarcoma and neuroblastoma (Supplementary Fig. 3).

In conclusion, we have validated a new immunoconjugate, EV20/Omomyc, which targets HER3 expressing MYCN addicted neuroblastoma cells. MYC members are potentially very important targets for paediatric embryonal tumours but developing direct inhibitors has been very challenging [34]. In this proof of principle study, we observed

significant therapeutic activity of the EV20/Omomyc immunoconjugate despite a DAR of 1, suggesting that the unconjugated antibody does not negatively affects the therapeutic activity of Omomyc. However, in view of a potential clinical development of the reagent, optimization of the conjugation efficiency and purification phase will be essential. The advantages of using Omomyc compared to other classical cyotoxic payloads are its low toxicity, high stability and broad anticancer activity based on its anti-MYC function. It will be interesting to investigate whether this new reagent can be effective against other paediatric solid tumours expressing HER3, such as medulloblastoma and rhabdomyosarcoma.

4. Material & Methods

4.1. Cell lines

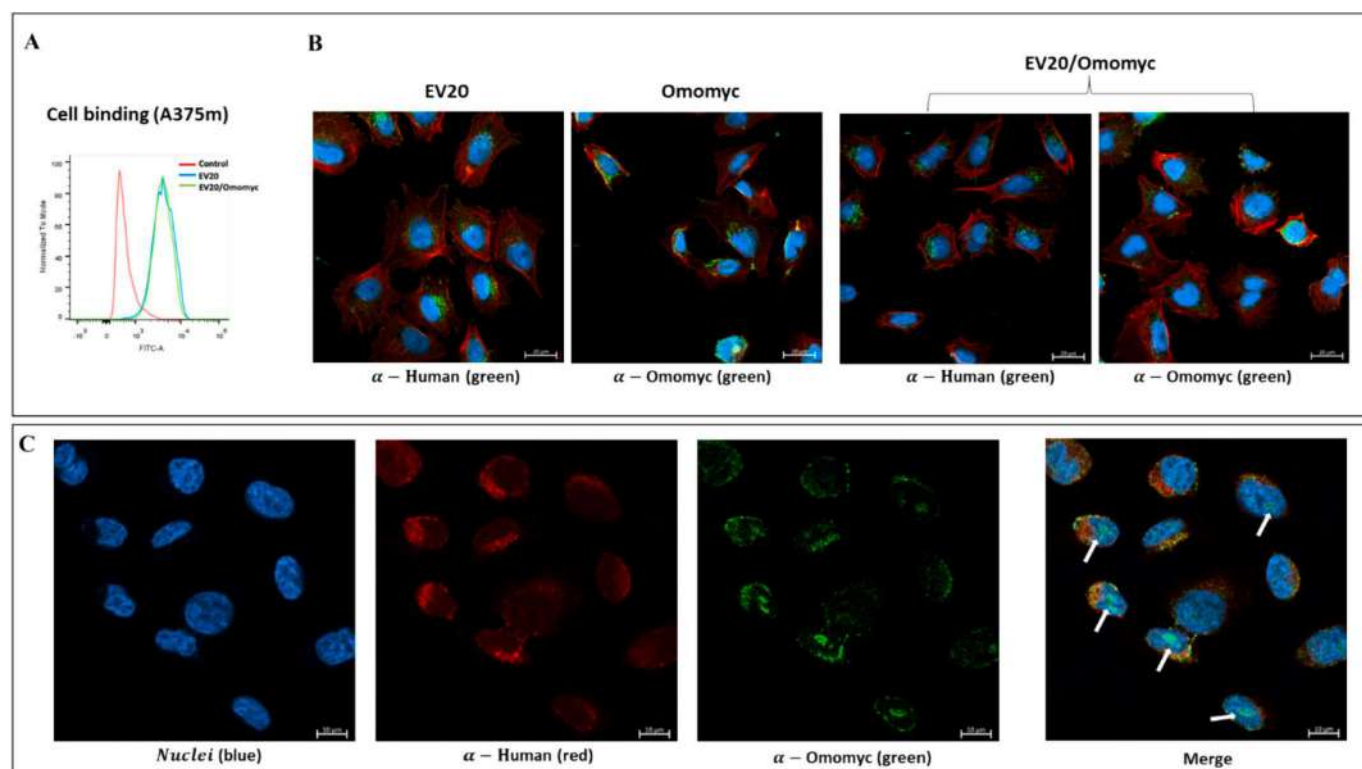Melanoma (A375m) and neuroblastoma (SKNAS, SH-SY5Y, SHEP,

Fig. 3. Cell binding and internalization of EV20/Omomyc in HER3+ melanoma cells.
(A) Cell binding analysis of EV20/Omomyc by flow cytometry of A375m melanoma cells; (B) Confocal images showing EV20/Omomyc internalization in A375m melanoma cells. Cells were treated for 4 h at 37 °C with 20 μg/ml for EV20 and EV20/Omomyc or with Omomyc (0.6 μg/ml), then fixed, permeabilized and stained with anti-human 488-conjugated secondary antibody or with murine anti-Omomyc antibody followed by anti-mouse 488-conjugated secondary antibody. Nuclei are visualized in blue with DAPI, actin is stained in red with TRITC-phalloidin; (C) Confocal imaging of EV20/Omomyc -treated A375m cells stained with anti-human 594-conjugated secondary antibody (EV20/red) and with murine anti-Omomyc antibody followed by anti-mouse 488-conjugated secondary antibody (Omomyc/green) showing Omomyc nuclear localization. Nuclei are visualized in blue with DAPI. White arrows indicate Omomyc nuclear localization.

SKNBE(2), SKSNH, GIMEN, IMR32) cells were purchased from American Type Culture Collection (Rockville, MD, USA). LAN-5 neuroblastoma cell line was purchased from Leibniz Institute DMSZ (German Collection of Microorganism and Cell Culture GmbH). Kelly neuroblastoma cell line was purchased from Sigma-Aldrich (St. Louis, MO, USA). Kelly-Mock and Kelly-HER3 cell lines were generated in our lab by lentiviral infection, as described below. All cell lines were cultured <3 months after resuscitation. The cells were cultured according to manufacturer's instructions, using a medium supplemented with 10% heat inactivated fetal bovine serum (FBS; Invitrogen, Carlsbad, CA, USA), L-glutamine, 100 units/ml penicillin, and 100 μg/ml streptomycin (Sigma-Aldrich Corporation, St. Louis, MO, USA), and incubated at 37 °C in humidified air with 5% CO_2. For patient-derived cell lines (COG-N-603; COG-N-636; COG-N-453; COG-N-496; COG-N-564), they were obtained from the Children's Oncology Group (COG) Cell Culture and Xenograft Repository at Texas Tech University Health Sciences Center (www.COGcell. org). Patient-derived cell lines were cultured in vitro using IMDM medium supplemented with 20% heat-inactivated fetal bovine serum (FBS; Invitrogen), 1% ITS (Insulin-Tranferrin-Selenium; Thermo Fisher Scientific, Waltham, MA, USA) 100 units/ml penicillin, and 100 μg/ml streptomycin (Sigma-Aldrich Corporation, St. Louis, MO, USA), and incubated at 37 °C in humidified air with 5% CO_2.

4.2. Generation of HER3 expressing neuroblastoma cell line

The vectors used for HER3 overexpression are the following: ErbB 3 (ERBB3) (NM_001982) Human Tagged Lenti ORF Clone (CAT#: RC209954L3; Origene, Rockville, Maryland, United States) cloned in a pLenti-C-Myc-DDK-P2A-Puro vector and pLenti-C-Myc-DDK-P2A-Puro Lentiviral Gene Expression Vector (CAT#: PS100092; Origene,

Rockville, Maryland, United States) for control Mock-Kelly cells. Lentiviruses were produced by transient cotransfection of a 3 plasmid expression system in the packaging 293 T cells, using lipofectamine 2000 (Invitrogen, Life Technologies). 293 T packaging cells were incubated for 8 h with the transfection reagents, then viral supernatant was collected 24 and 48 h after transfection and filtered through 0.45 μm pore vacuum sterile filtration system (Millipore, Life Science, Darmstadt, Germany). Then, Kelly cells were plated in a six-multiwell at a density of 125,000 cells/well, and they were subjected to 2 rounds of infections with 293 T filtered viral supernatant harvested 24 h and 48 h after transfection. To select for infected Kelly-HER3 and Kelly-Mock cells, puromycin was added to the media at the concentration determined in the steps above; one uninfected plate of cells in parallel was maintained in puromycin as a positive control for the puromycin selection.

4.3. Coomassie Staining

For characterization of the reagent, purified EV20 antibody, EV20/Omomyc or free Omomyc were resuspended in reducing or not reducing Laemmli Buffer and boiled for 10 min at 95 °C. Then they were separated by SDS/PAGE on 15% (non-reducing conditions, without 2-mercaptoethanol) or 8% (reducing conditions) polyacrylamide gel and Coomassie staining was performed. Briefly, gels were incubated with 50% (v/v) ethanol, 10% (v/v) acetic acid solution in water for fixing, then they were stained with 0.1% (w/v) Coomassie blue R350, 20% (v/v) methanol, and 10% (v/v) acetic acid solution in water, and finally destained with 50% (v/v) methanol in water with 10% (v/v) acetic acid.
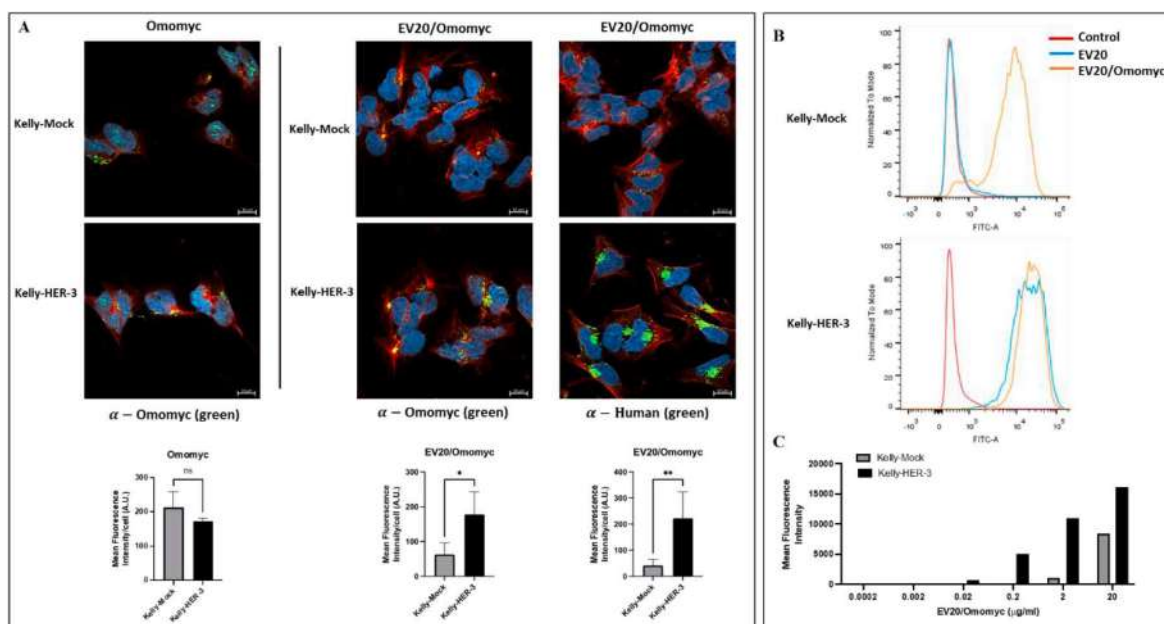
Fig. 4. Conjugation with the EV20 antibody increases Omomyc nuclear delivery in HER3 expressing Kelly neuroblastoma cells.

(A) Confocal images showing EV20/Omomyc internalization in Kelly-Mock and Kelly-HER3 neuroblastoma cells. Cells were treated for 4 h at 37 °C with (20 μg/ml) EV20/Omomyc or (2 μg/ml) Omomyc, then they are fixed, permeabilized and stained with anti-human 488-conjugated secondary antibody or with murine anti-Omomyc antibody followed by anti-mouse 488-conjugated secondary antibody. Nuclei are visualized in blue with DAPI, actin is stained in red with TRITC-phalloidin. Below histograms representing quantification of the internalization using mean fluorescence intensity of AF-488 in individual cells. Unpaired *t*-Test $*p = 0.01$; $**p = 0.002$ B) EV20/Omomyc cell binding on Kelly-Mock and Kelly-HER3 neuroblastoma cells by flow cytometry. EV20 antibody is used as control. Cells were stained with anti-human 488-conjugated secondary antibody and analysed by flow cytometry; (C) Titration of EV20/Omomyc on Kelly-Mock and Kelly-HER3 neuroblastoma cells. Cells were detached and treated with increasing doses of EV20/Omomyc at 4 °C for 30 min, washed and incubated with anti-human 488-conjugated secondary antibody, followed by flow cytometric analysis.
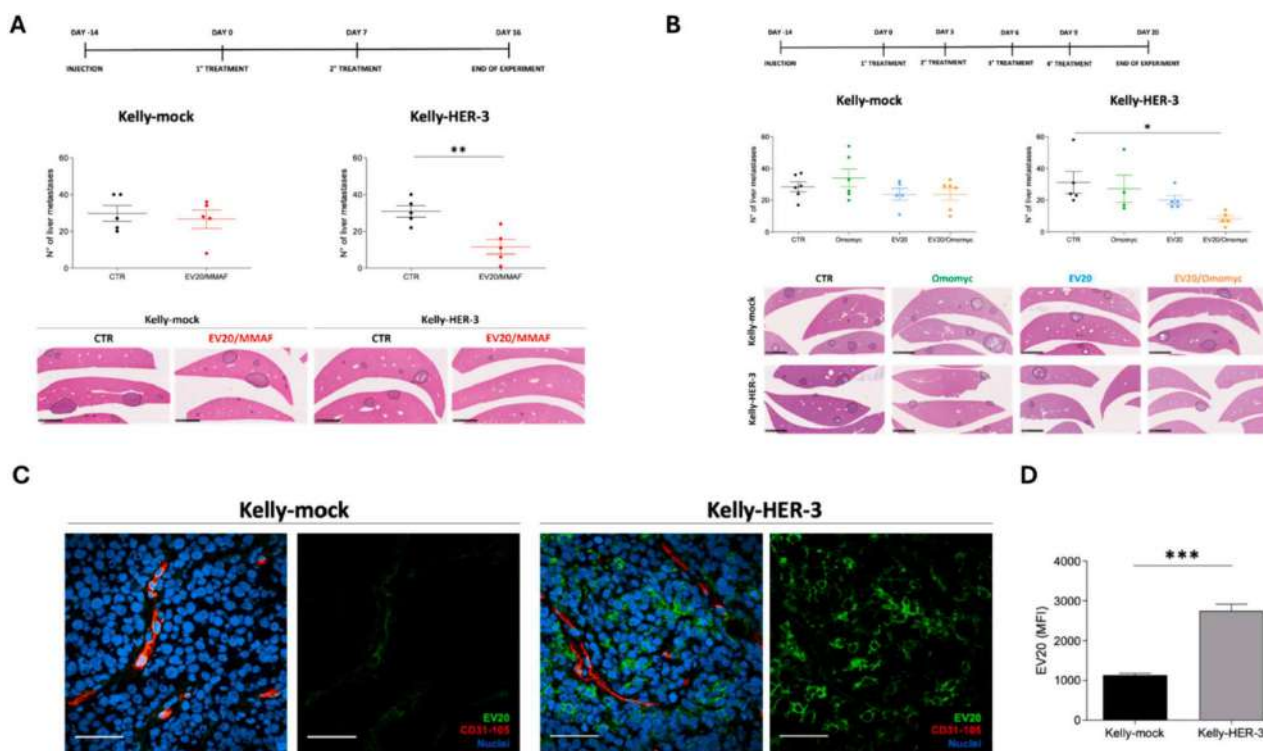

Fig. 5. ADC and EV20/Omomyc activity in Kelly pseudo-metastatic model.

4.4. Western Blotting

For characterization of the reagent, purified EV20 antibody, EV20/ Omomyc or free Omomyc were resuspended in reducing or not reducing Laemmli Buffer and boiled for 10 min at 95 °C. Then they were separated by SDS/PAGE on 15% (non-reducing conditions, without 2-

mercaptoethanol) or 8% (reducing conditions) polyacrylamide gel and transferred to nitrocellulose membrane. Membranes were blocked with 5% non-fat dry milk in PBS 0.1% Tween 20 for 1 h at room temperature and incubated with the following antibodies. For Omomyc detection it was used murine anti-Omomyc antibody (Ximbio, Anti-Omomyc [21−1−3]; 1:1000 dilution) overnight at 4 °C followed by goat anti-mouse IgG HRP-conjugated secondary antibody (Biorad, Berkeley, CA, USA; 1:10000 dilution) for 1 h at RT; for EV20 antibody detection it was used goat anti-human IgG-HRP-conjugated secondary antibody (#A01070, Sigma-Aldrich Corporation; 1:20000 dilution) for 1 h at RT. For cell lysates analysis, cells were lysed in RIPA Buffer (50 mM Tris-HCl, 1% NP40, 0.1% SDS, 150 mM NaCl) supplemented with protease inhibitor cocktail (Sigma-Aldrich) and phosphatase inhibitor cocktail (Roche) for 30 min in ice. Insoluble material was removed by centrifugation (13,000 rpm for 20 min at 4 °C) and protein concentration was assessed by Bradford assay. Equal amounts of protein were separated by SDS/PAGE on 15% or 8% polyacrylamide gel and transferred to nitrocellulose membrane. Membranes were blocked with 5% non-fat dry milk in PBS 0.1% Tween 20 for 1 h at room temperature and incubated overnight at 4 °C with primary antibodies. The primary antibodies used were: N-Myc (sc-53,993, Santa Cruz Biotechnology, 1:500 dilution), Max (#4739, Cell Signalling Technology, 1:1000 dilution), Actin (Sigma Aldrich Corporation, 1:40000 dilution), HER3/ErbB3 (#12708, Cell Signalling Technology 1:1000 dilution). After washing with PBS containing 0.1% Tween-20, blots were incubated with a goat anti-mouse IgG HRP-conjugated (Biorad, Berkeley, CA, USA; 1:20000 dilution) and an anti-rabbit IgG HRP-conjugated antibody (Biorad, Berkeley, CA, USA; 1:20000 dilution) as secondary antibodies, at room temperature for 1 h. Detection of signal bands was performed with Clarity Western ECL substrate (#1705061; Biorad, Hercules, CA, USA). Images of membranes were acquired with a Uvitec FireReader (Cambridge, UK).

4.5. MTT cell viability assay

Cytotoxicity was assessed by MTT [3-(4,5-dimethyldiazol-2-yl)-2,5-diphenyl tetrazolium bromide] assay. Cells were seeded into 96-well plates at a density ranging from 3.5×10^3 to 5×10^3 cells/well in 200 μl of complete culture medium and cultivated under standard growth conditions for 24 h at 37 °C in 5% CO2. Afterwards, cells were treated in complete medium with Omomyc 20 μM for 72 h, and with increasing doses of EV20/MMAF for 120 h. At the end of the incubation periods, cells were incubated with 100 μl of MTT solution [3-(4,5-dimethyldiazol-2-yl)-2,5-diphenyl tetrazolium bromide] (Sigma-Aldrich) (0.5 mg/ml of MTT in serum free medium) for 2 h at 37 °C. After removal of the MTT solution, cells were incubated with 100 μl of dimethyl sulfoxide (DMSO) for 10 min and the optical density was measured at 570 nm using a multi-plate reader. All experiments were performed in triplicate.

4.6. Patients

The study cohort was formed by 50 neuroblastoma (NB) patients diagnosed between 2012 and 2018 at IRCCS "G. Gaslini" Institute, Genoa, Italy. All patients gave written consent to the study. The study was approved by Chieti-Pescara Local Ethics Committee (E.C. number 06/07.04.2022). All patients gave written consent to the study. The median age of all patients was 23.5 months old (range, 2–88), and 60.3% of the NB patients (35 out of 58) were female. The clinical and pathological characteristics of NB patients are summarized in Table 2 (supplemental materials).

4.7. Immunohistochemistry

The expression study was performed on whole paraffin sections that were deparaffinized and prepared for the immunohistochemical staining with the anti-HER3 rabbit monoclonal antibody (clone SP-71; dilution

1:100) purchased from AbCam. Antigen retrieval was performed by microwave treatment at 750 W (10 min) in Tris-EDTA buffer (pH 8.0). The anti-rabbit EnVision kit (Agilent, K4003) was used for signal amplification. To exclude the unspecific staining, isotype control was included. In neuroblastoma cells, HER3 showed exclusive cytoplasmic immunohistochemical pattern. Briefly, the level of HER3 expression was obtained on a sum of the scored percentage of positive cells (i.e., <5%, score 0; 5–50%, score 1; >50%, score 2) and scored labeling (i.e., Negative, score 0; Faint, score 1; Moderate, score 2; Strong, score 3). The final HER3 expression level was categorized as "Negative" (i.e., Sum of scores: 0, 1), "Low-expression" (i.e., Sum of scores: 2, 3), or "High-expression" (i.e., Sum of scores: 4, 5).

4.8. Generation of EV20/Omomyc

EV20/Omomyc immunoconjugate was developed through the conjugation of Omomyc to EV20 antibody by means of a hetero-bifunctional linker reacting to amine residues on Omomyc (introducing a disulphide linker on the protein surface) and a second hetero-bifunctional reagent on EV20 (introducing a free -SH group) thus to favour the formation of intermolecular disulphide bridge between the 2 proteins.

To prepare the samples for the reaction, the EV20 antibody and reduced Omomyc were buffer exchanged to 100 mM Borate Buffered Saline pH 9 (BBS) with centrifugal filter units with cutoff 30 kda (for EV20) and 3 kda (for Omomyc). EV20 was chemically modified with 2-Iminothiolane (2-IT, Thermofisher, USA; stock dissolved in water) using 1.5 M excess of this reagent, while Omomyc was chemically modified with succinimidyl 3-(2-pyridyldithio)propionate (SPDP, SIGMA-Aldrich, USA; stock dissolved in DMSO) using 1.7 M excess of the reagent. Excess reagents were removed by gel filtration on a G25 column (GE Healthcare, USA) equilibrated in BBS buffer. Fractions containing the 2 proteins were collected, and EV20-2IT and Omomyc-SPDP were then mixed with 1:5 ratio respectively. The reaction for the formation of disulfide bond between EV20 and Omomyc was carried out over 2 h at room temperature, and monitored following the release of pyridine-2-thione at 343 nm by spectrophotometer. After the reaction, the mixture was concentrated to 5 mg/ml with a centrifugal filter unit of 30 kDa cutoff. Removal of Omomyc-2IT unreacted product was done on G25 (40 ml volume) column with FPLC in Phosphate Buffered Saline pH 7.4 (PBS) with an isocratic flow rate at 1.5 ml/min. Further residual Omomyc-2IT was then removed by ion exchange chromatography on a Q-Sepharose Column in 20 mM Trizma pH 9, eluting with PBS in isocratic flow rate (1 ml/min). Purified samples were analysed by western blotting using anti-Omomyc antibody (Ximbio, Anti-Omomyc [21–1-3]). DAR was assessed by mass spectrometry performed by Toscana Life Sciences (http://www.toscanalifesciences.org/it/). The naked EV20 and EV20/Omomyc were desalted using Spin Trap G25 (Cytiva). For each sample, 2 μL of the resulting solution was mixed with 2 μL of a saturated solution of s-DHB in 0.1% TFA in acetonitrile:water (50:50, *v/v*). The mixture was spotted onto the MALDI plate and left to dry in the air. Successively, 1 μL of the saturated matrix solution was added to each dried spot and it was let to dry again. A protein standard II calibration mixture from Bruker Daltonics (GmbH, Bremen, Germany) was used for the calibration procedure. The mass spectra were acquired over the mass range *m/z* 30–220 kDa, in linear mode, using an UltrafleXtreme (Bruker Daltonics, GmbH) MALDI mass spectrometer.

4.9. ELISA

For EV20/Omomyc in vitro binding assay, 96-well plates NUNC Maxisorp modules were coated with Recombinant HER-3 extracellular domain (ECD) (1 μg/ml) overnight at 4 °C. After blocking with 1% BSA in PBS at room temperature for 1 h, increasing concentrations of EV20/Omomyc or EV20 as control were added and incubated at room temperature for 1 h. After several washes with PBS + 0,05% Tween-20, a

goat anti-human IgG-HRP solution (Sigma-Aldrich Corporation) was added to each well and incubated at room temperature for 1 h. After washes, stabilized chromogen was added to each well for at least 10 min in the dark, then the reaction was stopped with the addition of 1 N H_2SO_4 and the resulting color read at 450 nm with an ELISA plate reader. For in vitro serum stability analysis, 37.5 μg of EV20/Omomyc was incubated in human serum at 37 °C for a period of time. Serum samples are drawn at different time points and the amount of conjugated antibody are measured using anti-Omomyc sandwich ELISA to calculate the degree of drug loss. In detail, 96-well plates NUNC Maxisorp modules were coated with murine anti-Omomyc antibody (0,5 μg/ml) overnight at 4 °C. After blocking with 1% BSA in PBS at room temperature for 1 h, increasing concentrations of EV20/Omomyc or EV20 as control were added and incubated at room temperature for 1 h. After several washes with PBS + 0,05% Tween-20, a goat anti-human IgG-HRP solution (Sigma-Aldrich Corporation) was added to each well and incubated at room temperature for 1 h. After washes, stabilized chromogen was added to each well for at least 10 min in the dark, then the reaction was stopped with the addition of 1 N H_2SO_4 and the resulting color read at 450 nm with an ELISA plate reader.

4.10. Confocal imaging

A375m, Kelly-Mock and Kelly-HER3 cells at 70% of confluence were grown on coverslips for 24 h and then incubated with EV20 (20 μg/ml), EV20/Omomyc (20 μg/ml) or Omomyc (2 or 0.6 μg/ml) for 4 h at 37 °C. Cells were then fixed in 4% paraformaldehyde for 15 min at room temperature, permeabilized with 0.25% Triton X-100 for 5 min, and blocked with goat serum 5% in PBS as blocking solution for 60 min at RT. Coverslips were then incubated overnight at 4 °C with murine anti-Omomyc antibody (Ximbio, Anti-Omomyc [21–1-3]; 1:100 dilution) followed by AlexaFluor-488 conjugated anti-mouse IgG 1:100 (A11017, Invitrogen, Life Technologies) 1 h at RT for Omomyc detection; and with AlexaFluor-488 conjugated anti-human IgG 1:100 (A11013, Invitrogen, Life Technologies) or AlexaFluor-594 conjugated anti-human IgG 1:100 (A11014, Invitrogen, Life Technologies) 1 h at RT for EV20 antibody detection. DAPI solution (P62248; Thermo Fisher Inc., Waltham, MA, USA) was used to visualize nuclei, actin is stained in red with TRITC-phalloidin and coverslips were mounted using ProLong Gold Antifade Mountant (P36930; Thermo Fisher Inc., Waltham, MA, USA). Confocal images were acquired using a Zeiss LSM800 inverted confocal microscope system (Carl Zeiss, Gottingen, Germany); detector gain voltages and pinhole were set at the beginning of the experiment and maintained constant during the acquisition of all samples. No significant fluorescent signal was detectable with the secondary antibodies alone. Fluorescence intensity of the internalized EV20/Omomyc or Omomyc was quantified using ImageJ Software, and normalized for DAPI-labelled cell nuclei.

4.11. FACS analysis

For HER3 surface expression analysis, A375m, Kelly-Mock and Kelly-HER3 cells were harvested and labelled with indicated doses of EV20/Omomyc or EV20 as control for 30 min on ice. After washing, cells were labelled with AlexaFluor-488 conjugated anti-human IgG (A11013, Invitrogen, Life Technologies) at a dilution of 1:300. Analysis was performed using a FACS Canto II cytometer (BD Biosciences).

4.12. Experimental Metastasis Assay

Immunodeficient NSG mice were purchased from Jackson Laboratory and bred in the animal facility of CAST, G. D'Annunzio University, Chieti. Animal care and experimental procedures were approved by the Ethics Committee for Animal Experimentation of the Institute according to Italian law (Authorization n° 292/2017-PR). 8-week old male NSG mice were injected via the lateral tail vein with 5×10^5 Kelly-Mock or Kelly-HER3 neuroblastoma cells; after 2 weeks, mice were randomly

divided into 2 groups that received PBS or EV20/MMAF (10 mg/Kg) weekly for a total of 2 doses or in 4 groups that received PBS, EV20 (5 mg/Kg), EV20/Omomyc (5 mg/Kg) and free Omomyc (0.6 mg/kg) weekly for a total of 4 doses. The animal health status was monitored daily, and body weight was measured once a week during the treatments. 11 days after last treatment mice were sacrificed and livers were harvested, fixed in 10% neutral buffered formalin, paraffin embedded, sectioned and stained with Hematoxylin and Eosin (Bio-Optica) for metastasis analysis. To optimize the detection of microscopic metastases and ensure systematic uniform and random sampling, livers were cut transversally into 2.0 mm thick parallel slabs with a random position of the first cut in first 2 mm of the organ, resulting in 6–8 slabs. The slabs were then embedded cut surface down and sections were stained with Hematoxylin and Eosin. Slides were independently evaluated by 2 pathologists to quantify the number of lesions. Sections were scanned with Nanozoomer scanner from Hamamatsu and images were acquired with NDP.view 2 software.

4.13. Immunofluorescence analysis of tumour xenografts

Xenografts were generated injecting subcutaneously into both flanks of mice a suspension of 5×10^6 Kelly-Mock and Kelly-HER3 cells in a total volume of 200 μl of PBS and Matrigel (ratio 1:1). When xenografts became palpable (approximately 100 mm³), animals received one single intravenous injection of EV20/Omomyc at the dose 10 mg/Kg, and were sacrificed 24 h later. Fresh tumour tissues were frozen in a crio-embedding medium (OCT, Bio-Optica) and cryostat sections were incubated with the following antibodies: AlexaFluor-488 conjugated anti-human IgG (A11013, Invitrogen, Life Technologies) in order to detect EV20 and rat monoclonal anti-CD31 (550,274, BD Pharmingen), mixed with rat monoclonal anti-CD105 (550,546, BD Pharmingen), followed by AlexaFluor-546 conjugated secondary antibody (A11081, Invitrogen, Life Technologies) in order to detect endothelial cells. Nuclei were stained with DAPI solution (Sigma). Images were acquired using Zeiss LSM 800 confocal microscope. Quantification of mean fluorescence intensity (MFI) of anti-human IgG was performed on digital images of 3 tumours per group (5×400 microscopic field per sample) using ZEN software.

4.14. Statistical analysis

For fluorescence intensity quantification and for metastasis analysis in Fig. 5A, *p* values were determined by unpaired Student's *t*-test and considered significant for $p < 0.05$. For metastasis analysis in Fig. 5B, one-way ANOVA statistical analysis with Tukey multiple comparison test was used to determine differences between treatment groups, * p < 0.05 indicates significant difference between the groups. All statistical analysis was performed with GraphPad Prism 5.0 software.

CRediT authorship contribution statement

Sandra Bibbo: Investigation, Data curation. **Emily Capone:** Investigation, Data curation. **Giulio Lovato:** Investigation, Methodology. **Sara Ponziani:** Investigation, Data curation. **Alessia Lamolinara:** Investigation, Data curation. **Manuela Iezzi:** Supervision, Data curation. **Rossano Lattanzio:** Investigation, Formal analysis. **Katia Mazzocco:** Validation, Formal analysis. **Martina Morini:** Validation, Formal analysis. **Francesco Giansanti:** Supervision, Methodology. **Vincenzo De Laurenzi:** Writing – review & editing, Supervision, Funding acquisition. **Jonathan Whitfield:** Writing – review & editing, Methodology, Data curation. **Stefano Iacobelli:** Writing – review &

Appendix A. Supplementary data

Supplementary data to this article can be found online at https://doi.org/10.1016/j.jconrel.2024.08.009.

References

[1] R. Dhanasekaran, et al., The MYC oncogene - the grand orchestrator of cancer growth and immune evasion, Nat. Rev. Clin. Oncol. 19 (2022) 23–36, https://doi.org/10.1038/s41571-021-00549-2.

[2] M. Conacci-Sorrell, L. McFerrin, R.N. Eisenman, An overview of MYC and its interactome, Cold Spring Harb. Perspect. Med. 4 (2014) a014357, https://doi.org/10.1101/cshperspect.a014357.

[3] R. Zeid, et al., Enhancer invasion shapes MYCN-dependent transcriptional amplification in neuroblastoma, Nat. Genet. 50 (2018) 515–523, https://doi.org/10.1038/s41588-018-0044-9.

[4] D. Masso-Valles, L. Soucek, Blocking Myc to treat Cancer: reflecting on two decades of Omomyc, Cells 9 (2020), https://doi.org/10.3390/cells9040883.

[5] M.E. Beaulieu, et al., Intrinsic cell-penetrating activity propels Omomyc from proof of concept to viable anti-MYC therapy, Sci. Transl. Med. 11 (2019), https://doi.org/10.1126/scitranslmed.aar5012.

[6] L. Soucek, et al., Modelling Myc inhibition as a cancer therapy, Nature 455 (2008) 679–683, https://doi.org/10.1038/nature07260.

[7] J.M. Vicencio, et al., Osimertinib and anti-HER3 combination therapy engages immune dependent tumor toxicity via STING activation in trans, Cell Death Dis. 13 (2022) 274, https://doi.org/10.1038/s41419-022-04701-3.

[8] M. Momeny, et al., Heregulin-HER3-HER2 signaling promotes matrix metalloproteinase-dependent blood-brain-barrier transendothelial migration of human breast cancer cell lines, Oncotarget 6 (2015) 3932–3946, https://doi.org/10.18632/oncotarget.2846.

[9] R. Ghasemi, et al., Dual targeting of ErbB-2/ErbB-3 results in enhanced antitumor activity in preclinical models of pancreatic cancer, Oncogenesis 3 (2014) e117, https://doi.org/10.1038/oncsis.2014.31.

[10] G. Sala, et al., EV20, a novel anti-ErbB-3 humanized antibody, promotes ErbB-3 Down-regulation and inhibits tumor growth in vivo, Transl. Oncol. 6 (2013) 676–684, https://doi.org/10.1593/tlo.13475.

[11] G. Sala, et al., An ErbB-3 antibody, MP-RM-1, inhibits tumor growth by blocking ligand-dependent and independent activation of ErbB-3/Akt signaling, Oncogene 31 (2012) 1275–1286, https://doi.org/10.1038/onc.2011.322.

[12] P.R. Prasetyanti, et al., ErbB-3 activation by NRG-1beta sustains growth and promotes vemurafenib resistance in BRAF-V600E colon cancer stem cells (CSCs), Oncotarget 6 (2015) 16902–16911, https://doi.org/10.18632/oncotarget.4642.

[13] D. D'Agostino, et al., EV20ssvc/MMAF, an HER3 targeting antibodydrug conjugate displays antitumor activity in liver cancer, Oncol. Rep. 45 (2021) 776–785, https://doi.org/10.3892/or.2020.7893.

[14] E. Capone, et al., EV20/NMS-P945, a novel Thienoindole based antibody-drug conjugate targeting HER-3 for solid tumors, Pharmaceutics 13 (2021), https://doi.org/10.3390/pharmaceutics13040483.

[15] L. Gandullo-Sanchez, et al., HER3 targeting with an antibody-drug conjugate bypasses resistance to anti-HER2 therapies, EMBO Mol. Med. 12 (2020) e11498, https://doi.org/10.15252/emmm.201911498.

[16] E. Capone, et al., EV20-mediated delivery of cytotoxic auristatin MMAF exhibits potent therapeutic efficacy in cutaneous melanoma, J. Control. Release 277 (2018) 48–56, https://doi.org/10.1016/j.jconrel.2018.03.016.

[17] E. Capone, et al., EV20-sap, a novel anti-HER-3 antibody-drug conjugate, displays promising antitumor activity in melanoma, Oncotarget 8 (2017) 95412–95424, https://doi.org/10.18632/oncotarget.20728.

[18] P. Varlet, et al., Comprehensive analysis of the ErbB receptor family in pediatric nervous system tumors and rhabdomyosarcoma, Pediatr. Blood Cancer 69 (2022) e29316, https://doi.org/10.1002/pbc.29316.

[19] E. Izycka-Swieszewska, et al., Expression and significance of HER family receptors in neuroblastic tumors, Clin. Exp. Metastasis 28 (2011) 271–282, https://doi.org/10.1007/s10585-010-9369-1.

[20] R. Ho, et al., Proliferation of human neuroblastomas mediated by the epidermal growth factor receptor, Cancer Res. 65 (2005) 9868–9875, https://doi.org/10.1158/0008-5472.Can-04-2426.

[21] B. Qiu, K.K. Matthay, Advancing therapy for neuroblastoma, Nat. Rev. Clin. Oncol. 19 (2022) 515–533, https://doi.org/10.1038/s41571-022-00643-z.

[22] K.C. Goldsmith, et al., Lorlatinib with or without chemotherapy in ALK-driven refractory/relapsed neuroblastoma: phase 1 trial results, Nat. Med. 29 (2023) 1092–1102, https://doi.org/10.1038/s41591-023-02297-5.

[23] L.L. Wang, et al., Augmented expression of MYC and/or MYCN protein defines highly aggressive MYC-driven neuroblastoma: a Children's oncology group study, Br. J. Cancer 113 (2015) 57–63, https://doi.org/10.1038/bjc.2015.188.

[24] M. Bansal, A. Gupta, H.F. Ding, MYCN and metabolic reprogramming in neuroblastoma, Cancers (Basel) 14 (2022), https://doi.org/10.3390/cancers14174113.

[25] E. Izycka-Swieszewska, et al., Expression and significance of HER family receptors in neuroblastic tumors, Clin. Exp. Metastasis 28 (2011) 271–282, https://doi.org/10.1007/s10585-010-9369-1.

[26] E. Capone, et al., HER-3 surface expression increases in advanced colorectal cancer representing a potential therapeutic target, Cell Death Dis. 9 (2023) 400, https://doi.org/10.1038/s41420-023-01692-8.

[27] E. Capone, et al., Targeting vesicular LGALS3BP by an antibody-drug conjugate as novel therapeutic strategy for neuroblastoma, Cancers (Basel) 12 (2020), https://doi.org/10.3390/cancers12102989.

[28] S. Bibbo, et al., Repurposing a psychoactive drug for children with cancer: p27 (Kip1)-dependent inhibition of metastatic neuroblastomas by Prozac, Oncogenesis 9 (2020) 3, https://doi.org/10.1038/s41389-019-0186-3.

[29] M.-E. Beaulieu, et al., Abstract 3435: identification of potential biomarkers of response to OMO-103, a first-in-modality pan-MYC inhibitor, in patients with advanced solid tumors, Cancer Res. 83 (2023) 3435, https://doi.org/10.1158/1538-7445.AM2023-3435.

[30] L. Gandullo-Sánchez, A. Ocaña, A. Pandiella, HER3 in cancer: from the bench to the bedside, J. Exp. Clin. Cancer Res. 41 (2022) 310, https://doi.org/10.1186/s13046-022-02515-x.

[31] H. Lyu, A. Han, E. Polsdofer, S. Liu, B. Liu, Understanding the biology of HER3 receptor as a therapeutic target in human cancer, Acta Pharm. Sin. B 8 (2018) 503–510, doi:https://doi.org/10.1016/j.apsb.2018.05.010.

[32] R. Hartley, T.N. Phoenix, MYC promotes aggressive growth and metastasis of a WNT-medulloblastoma mouse model, Dev. Neurosci. (2023), https://doi.org/10.1159/000533270.

[33] J. Ommer, et al., Aurora a kinase inhibition destabilizes PAX3-FOXO1 and MYCN and synergizes with Navitoclax to induce rhabdomyosarcoma cell death, Cancer Res. 80 (2020) 832–842, https://doi.org/10.1158/0008-5472.Can-19-1479.

[34] T. Shalaby, M.A. Grotzer, MYC as therapeutic target for embryonal tumors: potential and challenges, Curr. Cancer Drug Targets 16 (2016) 2–21, https://doi.org/10.2174/1568009615666150916092745.